Comparison of Fouling Mechanisms of Four Nanofiltration Membranes: Optimal Membrane Selection for Stephenfield Regional WTP, MB, Canada

I. Moran*, B. Gorczyca
University of Manitoba Department of Civil and Environmental Engineering, University of Manitoba, 15 Gillson St. Winnipeg, Manitoba, Canada, R3T 5V6.

Corresponding Author* Email: ummorani@umanitoba.ca

Abstract: Dual membrane filtration plants, incorporating microfiltration (MF) and nanofiltration (NF) have become widely used in potable water treatment as a method that can meet increasingly stringent THMs standards. Due to the high soluble material content in Manitoba and surrounding areas, a major concern for plant optimization is NF fouling. Over operational time, the foulant layer acts as an inhibitor of permeate flux and can significantly decrease membrane element longevity and increase plant operational cost. The extent of membrane fouling is determined by the specific interaction between the membrane and soluble material in the feed water. A detailed understanding of NF fouling mechanisms is necessary to optimize plant operation. Physical and chemical analyses were carried out on four different membranes (DOW FILMTEC NF90-400/34i, DOW FILMTEC NF270-400/34i, DOW FILMTEC BW30XFR-400/34i, DOW FILMTEC XFRLE-400/34i) to determine the optimal membrane for installation in the Stephenfield Regional WTP in southern Manitoba. Post-MF water from the Stephenfield Regional WTP was run in cross flow at 10bar (145psi) across each membrane at different operational time steps (1, 4, 12, 24, 48 hours). Virgin membrane surface roughness appears to be the governing factor for the degree and mechanism of fouling. Atomic force microscopy showed the initially rough NF90 and BW30 membranes experience a higher initial rate of fouling due to the higher surface area to attach and surface contours for soluble material to grab. The non-fouling resistant NF90 and NF270 membranes experienced a flux restoration from fouling over time. This phenomenon is predicted to be the dual result of membrane compaction and scouring. The flattening process of membrane peaks pulls down the overbearing layer of foulant causing an increase in surface roughness with greater susceptibility to the effects of cross flow scouring. The BW30 and XLE, coated with a fouling-resistant polyether block amide compound, experienced a lesser degree of fouling. The retained mass of foulant on the NF90 was three times greater than the other tested membranes due to the high virgin membrane surface roughness and lack of fouling resistant coating. This understanding of fouling mechanisms, as well as permeate quality, was used to select the NF270 as the optimal element for longevity and operational cost.

Keywords: Membrane Fouling; Plant Optimization; High Soluble Material Content

INTRODUCTION

Motivation

In a water treatment plant (WTP), membrane filtration is used as a water treatment process to remove particulate and dissolved material in water to improve the quality of water prior to distribution. Over operational time, this particulate and dissolved material builds up on the surface of a membrane and can have important implications regarding flux (flow rate) and material removal efficiency, among others. An understanding of fouling mechanisms and behavior can be used to predict the short- and long-term consequences of fouling or to make an informed decision as to which membrane, within a set of membranes, is most capable of withstanding the effects of fouling for a particular raw water source. For a water treatment plant, this can be important to meet both the demands of the client and federal and provincial water quality standards. This thesis investigates the relationship between four nanofiltration membranes and raw water from the Stephenfield Regional WTP in southern Manitoba and to make an informed decision as to which membrane is most suitable for installation in the Stephenfield Regional WTP.

Literature Review

The membrane selection process is fundamental to long-term plant cost and operation. A membrane that experiences a faster rate of fouling due to surface morphology, hydrophobicity or other key properties may not be the optimal choice for installation. Vrijenhoek et al. discuss the influence of membrane surface properties on the initial rate of colloidal fouling of reverse osmosis and nanofiltration membranes. The conducted research compares the fouling mechanisms of two nanofiltration membranes (Osmonics HL, Dow-FilmTec NF-70) and two reverse osmosis membranes (Trisep X-20, Hydkronautics LFC-1) [Vrijenhoek et al. (2001)].

The four tested membrane showed vastly different virgin membrane surface roughness. Compared to the relatively smooth HL membrane, the X-20, NF-70 and LFC-1 had surface roughnesses approximately three, four and five times greater than the HL membrane, respectively. The experiment conducted by Vrijenhoek et al. compared the decline in flux of each of these membranes to the relative surface roughness and a 0.99 positive correlation coefficient was determined between these two variables. The strong positive correlation between initial surface roughness and flux decline is a result of what the authors describe as “valley clogging” which is further supported by three-dimensional surface scans taken by atomic force microscopy. In its context, valley clogging refers to the rapid deposition of material in the valleys of an initially rough membrane which causes a rapid increase in foulant mass and subsequent decline in flux. This phenomenon is less prominent in membranes with low initial roughness as there are fewer valleys to get caught in and less surface area to attach. The reasonability of the concept of valley clogging, supported by a strong correlation between it and early flux decline, may be important in the membrane selection process. This data puts an asterisk on the “time zero” permeate flux and may shift our attention to the permeate flux after sufficient valley clogging has occurred.

Virgin membrane zeta potential was considered as a proponent of initial fouling. Zeta potential is likely only a significant factor when parts of the membrane surface are exposed. In other words, zeta potential will have a stronger impact regarding foulant-on-membrane fouling rather than foulant-on-foulant fouling. Flux decline was normalized to the membrane with the smallest decline in flux, the HL membrane, and compared with zeta potential. All other variables held constant, the correlation coefficient between these two variables was 0.05. This small correlation coefficient suggests a weak correlation between zeta potential and the four tested membranes in the study. It is important to note than none of the membranes in this study are coated with a polyether block amide compound – any one of several commercially available amide coatings which alters the electrostatic properties of the uppermost layer of the membrane resulting in the repulsion of common fouling material. This experiment has demonstrated the lack of correlation between virgin membrane zeta potential and the two reverse osmosis and two nanofiltration membrane in the study. Further investigation may be necessary to determine any correlation between zeta potential and membranes coated with a polyether block amide compound.

Salt rejection is a measure of the passage of dissolved salts past the surface of a membrane. The four tested membranes were subjected to a silica dose of 200mg/L in operation for the two hours and the initial and final salt concentrations were compared. The resultant correlation coefficient between flux decline and salt rejection was 0.87. In this experiment, the X-20 and LFC-1 membranes had the same salt rejection, but a nearly twofold difference in normalized flux decline. Due to the similarities in salt rejection between these two membranes, Vrijenhoek et al. suggest a coincidental relationship between salt rejection and flux decline and rather focuses on the relationship between salt rejection and virgin membrane surface roughness; the rough initial surface of the membrane causes rapid deposition of the water containing a high concentration of the soluble salt particles. While it is not directly stated in this report, it is expected that the major proponent of salt rejection is relative pore size or molecular weight cut-off. This is supported by the manufacturer-specified salt rejection of the LFC-1 and X-20 having the same value of 99.0% and experimentally rejecting the same amount of salt. The relationship between salt rejection and surface roughness is explained in more detail in Section 1.2.1 of this report.

The experiments conducted by Vrijenhoek et al. provide readers with a basic understanding of reverse osmosis and nanofiltration membrane fouling mechanisms. The report emphasizes the impact of virgin membrane surface roughness in the early stages of fouling – fouling is more rapid for membranes with high virgin surface roughness due to high friction between the membrane and soluble material by what the author describes as “valley clogging”. This idea is supported by data showing a strong correlation between surface roughness and flux decline. The report shows an insignificant correlation between membrane hydrophobicity and flux decline and what the author describes as a coincidental relationship between salt rejection and flux decline.

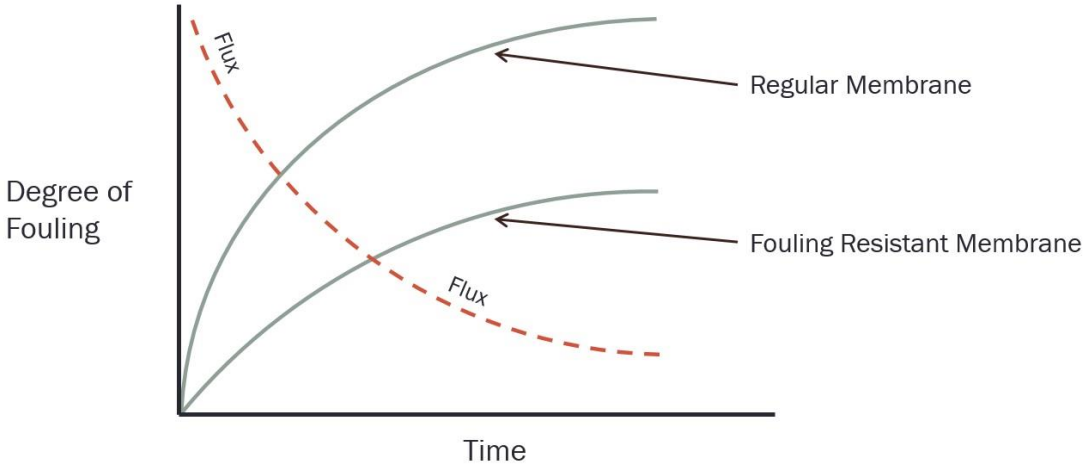
While this report effectively shows the relationship, or lack thereof, between flux decline and the aforementioned parameters, there are still properties that either require further investigation or that are not covered. The membranes used in this research were made of different material, but were not coated with a polyether block amide compound – a developing membrane property generally used against waters of high soluble material content as a way to avoid fouling [Jiraratananon et al. (2002)]. The effects of these polyether block amide compounds, found commercially through different membrane manufacturers, may be of particular interest. In addition, the experiment isolated the effects of membrane compaction by subjecting the

membrane sample to 24 hours at normal operating pressures for 24 hours prior to testing. While membrane compaction is not part of the scope of this study, it may be important in developing a more complete understanding of the membrane properties over time; there may be a relationship between membrane compaction and early membrane fouling under typical operating conditions.

Effects of Membrane Fouling

Over operational time, the amount of foulant retained on the surface of a membrane increases and prevents the passage of permeate across the membrane by "flux inhibition" [Mallevialle et al. (1996)]. This mechanism can be seen in Figure 1. Controlling the permeate flux can be of great importance for WTP operators in order to meet the demand of customers. Increasing pressure in the filtration system can increase the permeate output, but can have negative energy consumption (cost) implications. Finding the optimal balance between these two parameters, supplemented by the cost and effectiveness of pre-treatment, is imperative for treatment plants to meet their cost goals [Schäfer et al. (2001)]. Depending on the classification of membrane, treatment plants can either use a backwashing cycle to remove the attached foulant or use chemical cleaning agents to restore flux. Membrane flux may not be fully restored to its original condition due to irreversible fouling – fouling that is strongly bound to the membrane and cannot be removed by backwashing or chemical cleaning [Kimura et al. (2004)] – but can help increase permeate output and membrane longevity.

Figure 1: The typical relationship between degree of fouling and flux over operational time for regular and fouling resistant membranes.

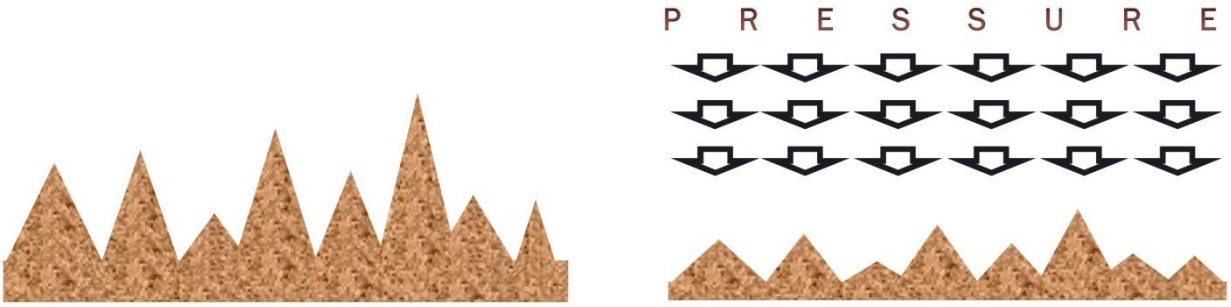


Effects of Membrane Compaction

Membrane compaction is a naturally occurring process in membrane filtration in which the surface contours or peaks are flattened by an applied pressure. This is an irreversible process that occurs in the early service life of a membrane and the effects quickly level off to a relative maximum. The degree of compaction is proportional to the applied pressure. The permanent flattening of peaks results in a permanent reduction in surface area which, in turn, causes an

overall reduction in flux [Persson et al. (1995)]. An illustration of membrane compaction can be seen in Figure 2.

Figure 2: a) A virgin membrane with high initial surface roughness and b) the same membrane after an applied pressure for a given amount of time.



a) b)

Fouling Resistant Membranes

Some membranes are coated with a polyether block amide compound, known commercially under the trademark name PEBAX®. Many commercially available nanofiltration membranes from DOW Chemical and Process are labeled as 'fouling resistant' as a result of this extra coating. Louie et al. showed that membranes coated in PEBAX® 1657 exhibited a decrease in surface roughness by 35-63%, a reduction of permeate flux by 29-81% and no significant change in hydrophilicity [Louis et al. (2006)]. Membranes with this attribute are often used in treatment of water with high salt content, such as brackish or sea water, and generally have a higher rejection of dissolved material. A simple comparison in fouling between a regular membrane and one coated with a polyether block amide compound can be seen in Figure 1.

METHODOLOGY

Membrane Selection Considerations

The Stephenfield Regional WTP in southern Manitoba is upgrading their water treatment system from chemical coagulation to a dual microfiltration and nanofiltration membrane filtration system. The need for this upgrade is due to the inefficiency of the chemical coagulation to remove DOC. This high DOC has resulted in failure of the effluent to meet the provincial and federal drinking water guidelines for trihalomethanes (THMs). It is expected that replacing the existing system with dual membrane filtration will enhance Stephenfield's removal efficiency of DOC and reduce the trihalomethane formation potential (THMFP).

Stephenfield Regional WTP Pilot-Scale Set-Up

The pilot-scale membrane filtration system at the Stephenfield Regional WTP is to simulate the performance of membranes to be installed in the full-scale operation. A schematic of the pilot-scale plant can be seen in Figure 3. Surface water is collected from the Boyne river and transferred to a chemical precipitation contact tank. The water is then pumped into the microfiltration system containing a single microfiltration element. Concentrate water from the microfiltration system is discarded into the drainage system. Post-microfiltration water is pumped into a secondary transfer tank before pumped into the reverse osmosis/nanofiltration system. The nanofiltration system contains three nanofiltration elements (Stage 1, Stage 2, Stage 3) ran in series. Permeate is collected at each stage and blended together to produce the plant's final effluent. Concentrate water from the nanofiltration system is discarded in the drainage system. The microfiltration and nanofiltration elements can be swapped out for new elements at the discretion of the plant operators.

Experimental Design Basis

Four nanofiltration membranes were chosen for small-scale testing. These membranes include the Dow FilmTec NF90-400/34i, Dow FilmTec NF270-400/34i, Dow FilmTec BW30XFR-400/34i and Dow FilmTec XFRLE-400/34i. Supplier-provided characteristics of these membranes can be seen in Table 1.

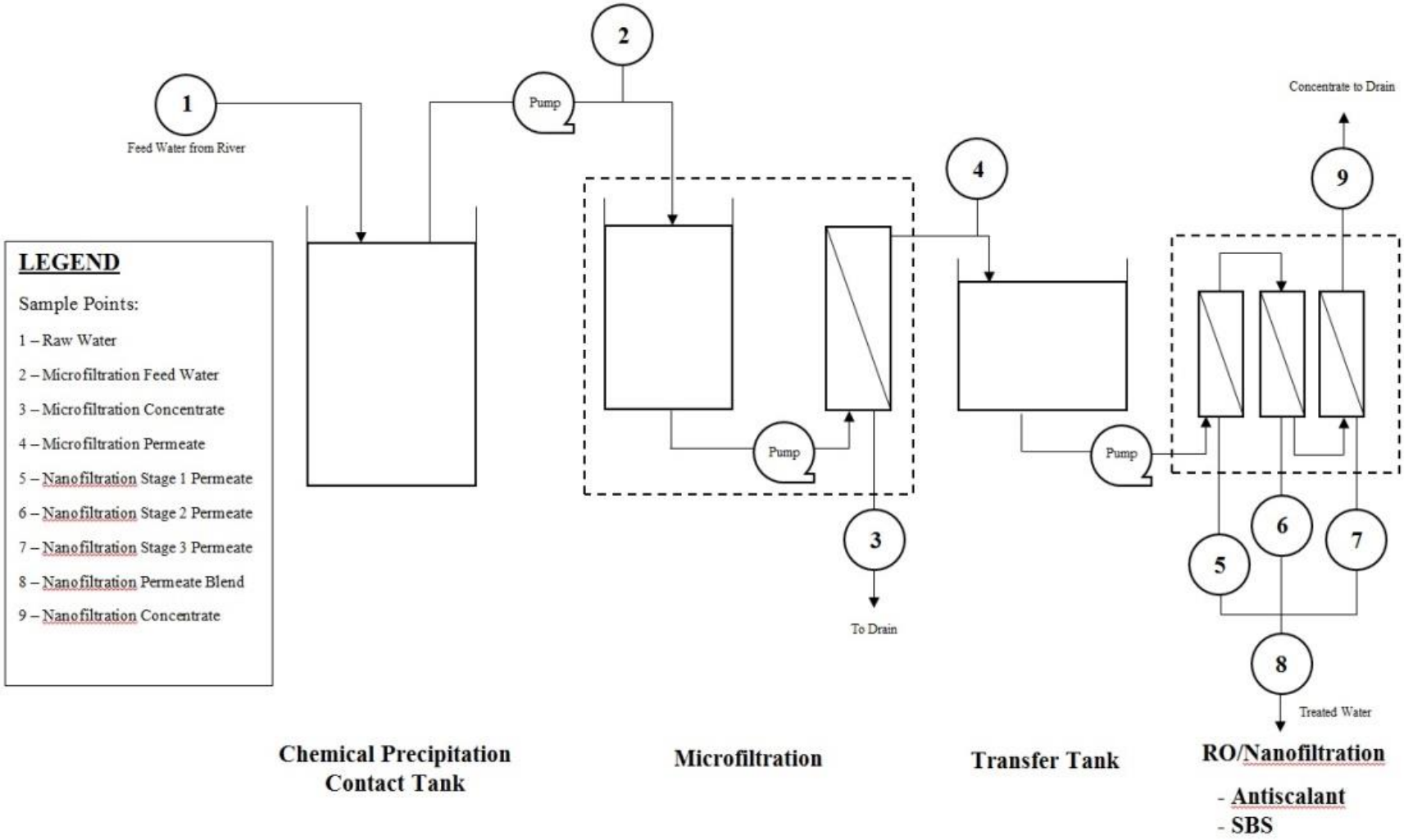
Table 1: Manufacturer-specified membrane attributes.

	NF90	NF270	BW30	XLE
Composition	Polyamide Thin-Film Composite	Polypiperazine Thin-Film Composite	Polyamide Thin-Film Composite	Polyamide Thin-Film Composite
Salt Rejection	Moderate	Moderate-High	High	High
Other Attributes	High Productivity	High Productivity	Brackish Water Fouling Resistant	Brackish Water Fouling Resistant Extra Low Energy

Bench-Top Membrane Filtration System

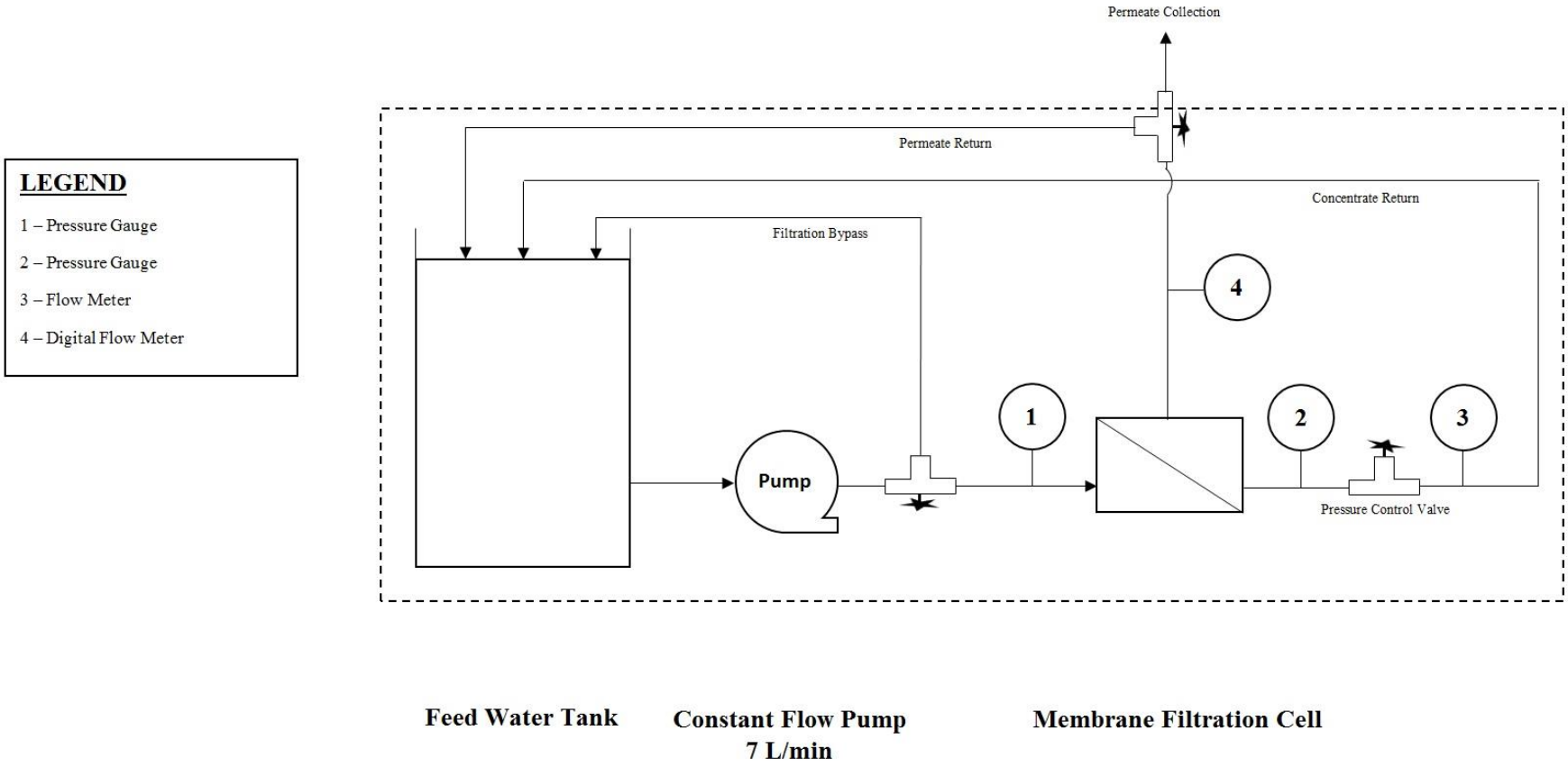
A custom bench-top membrane filtration system was used to carry out the small-scale testing. 75L of post-microfiltration water from the Stephenfield Regional WTP and placed in a 125L Equinox feed tank. Feed water was pumped through a WEG Hydra-Cell constant flow pump forcing 7L/min through the system. Water was pumped into a Sterlitech CF042 membrane filtration cell and ran in crossflow across the surface of the encased membrane. Depending on the needs of the experiment, permeate is either collected for analysis or recycled back into the feed tank. A flow diagram of the experimental setup can be seen in Figure 4.

Figure 3: Flow chart for the pilot-scale membrane filtration system at the Stephenfield Regional WTP, MB, Canada.



[7]

Figure 4: Flow chart for the bench-top membrane filtration system at the University of Manitoba.



Operating Conditions and Measurements

Membrane partitions were cut from a flat sheet membrane sample to an approximate size of 4.25x9cm and placed in a 10% methanol-in-water solution for 24 hours prior to filtration. Each NF membrane was ran in the bench-top membrane filtration system for 1, 4, 12 and 24 hours. Pressure was held constant at 10bar (145psi) for all trials. Flux measurements were taken at the intervals specified in Table 2. Membranes were removed from the filtration cell and placed in a sealed beaker containing DI water until subsequent testing.

Table 2: Flux measurement recording schedule.

Time [min]	Interval [min]
0 - 10	1
10 - 20	2
20 - 60	5

Removal Efficiency of Raw Water Characteristics

Characteristics of the feed water will be compared to the permeate characteristics to determine the removal efficiency of dissolved constituents. Testing for manganese will be carried out in accordance to ASTM D858-12 Standard Test Methods for Manganese in Water, testing for iron in accordance with ASTM D1068-10 Standard Test Methods for Iron in Water, testing for alkalinity in accordance with ASTM D1067-11 Standard Test Methods for Acidity or Alkalinity in Water and testing for hardness in accordance with ASTM D1126-12 Standard Test Method for Hardness in Water. Measurements for DOC were taken using a Teledyne Tekmar TOC Fusion TOC Analyzer.

Characteristics of Membrane and Foulant by Chemical and Oxidative Testing

Chemical and oxidative testing was carried out to show the change in membrane and foulant characteristics over time. Three drops of methylene blue dye were placed on the active surface of the fouled membrane and left for ten seconds. The dye was rinsed off with deionized water and dye absorbance was noted. On a separate partition, three drops of 0.1N hydrochloric acid was placed on the active surface of the membrane. The presence of any effervescence indicates the presence of carbonates in the foulant. The Fujiwara test was performed on a third membrane partition. A solution was prepared with 2mL of 0.1N sodium hydroxide and 1mL of pyridine. The membrane partition was placed in the solution and gently heated over a standard Bunsen burner. A change in color to pink indicated the presence of oxidizing halogens in the foulant.

Surface Complexity

The change in surface complexity over time was measured by two distinct methods. The effects of membrane compaction were monitored by subjecting each membrane to the same tests prescribed above, but filtered instead with deionized water in crossflow across the surface of the membrane. As membrane compaction is a direct result of applied pressure, the decline in flux is directly proportional to the decline in surface area.

A Veeco Dimension 3100 atomic force microscope with a NanoScope IVa Controller was used to show the change in foulant complexity over time. A 100µm^2 surface area was plotted in contact mode at a speed of 10µm/s. Relative surface roughness and three-dimensional surface images were collected for analysis.

RESULTS AND DISCUSSION

Filtration Influent Water Quality

Table 3: Post-microfiltration / nanofiltration feed water from the Stephenfield Regional WTP. Collection date: July 8th, 2015.

Analyte	Concentration
Alkalinity (mg/L $CaCO_3$)	501
pH	8.13
Hardness (mg/L $CaCO_3$)	360
Total Organic Carbon (mg/L)	18.6
Manganese (mg/L)	1.807
Iron (mg/L)	0.78
Conductivity (mS/cm)	1.152

Removal Efficiency of Raw Water Characteristics

Manitoba surface waters are characterized by very high levels of DOC, making its removal an important consideration to reduce the THM formation potential. Removal efficiencies of DOC< hardness, alkalinity and manganese can be seen in Figures 5 through 8. All membranes effectively removed over 98% DOC by the late stage. The NF270 was the only membrane to leave a significant residual of hardness, alkalinity and manganese at roughly 20% each. This residual hardness and alkalinity may be desirable to avoid post-treatment addition of hardness, but the residual manganese may cause the plant to fail to meet its target residual manganese. This residual is likely a reflection of the molecular weight cut-off (relative indication of pore size), but may also be attributed to the different membrane material; the NF270 is a polypiperazine thin-film composite. Further investigation as to the impact of different membrane material will be completed at a later date.

Figure 5: The lab-simulated removal efficiency of DOC at stage 1 and stage 3.

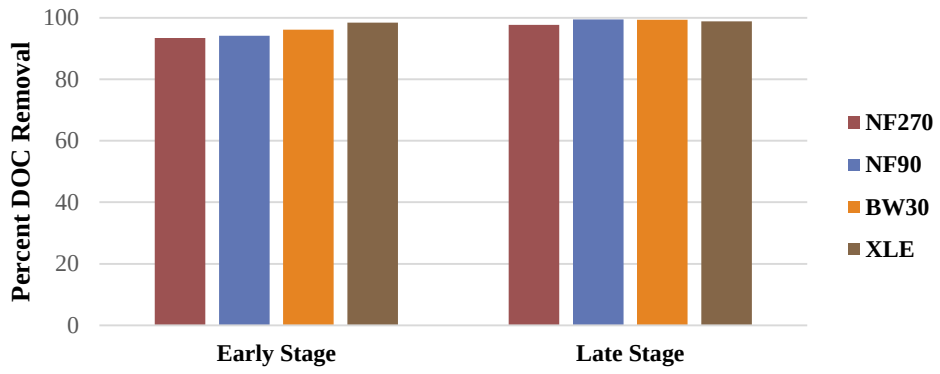


Figure 6: The lab-simulated removal efficiency of hardness at stage 1 and stage 3.

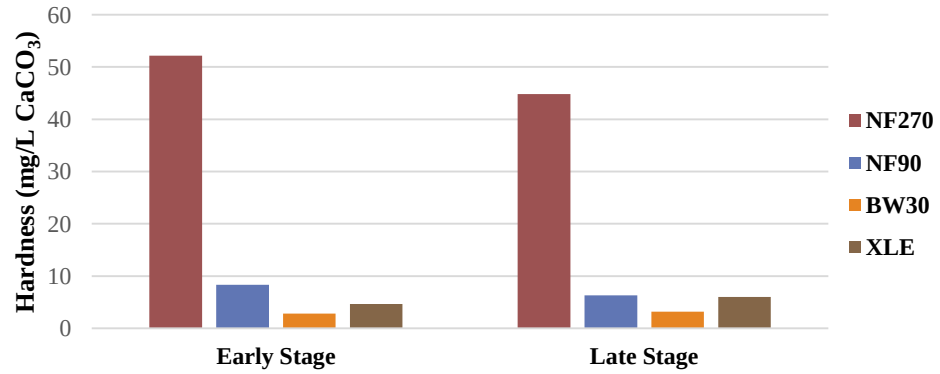


Figure 7: The lab-simulated removal efficiency of alkalinity at stage 1 and stage 3.

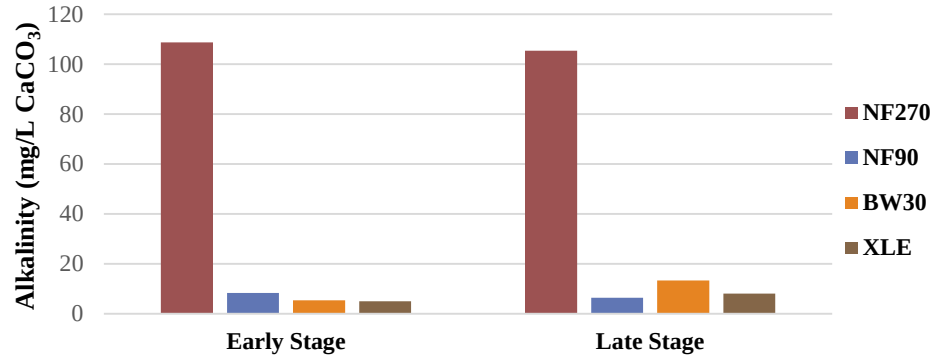
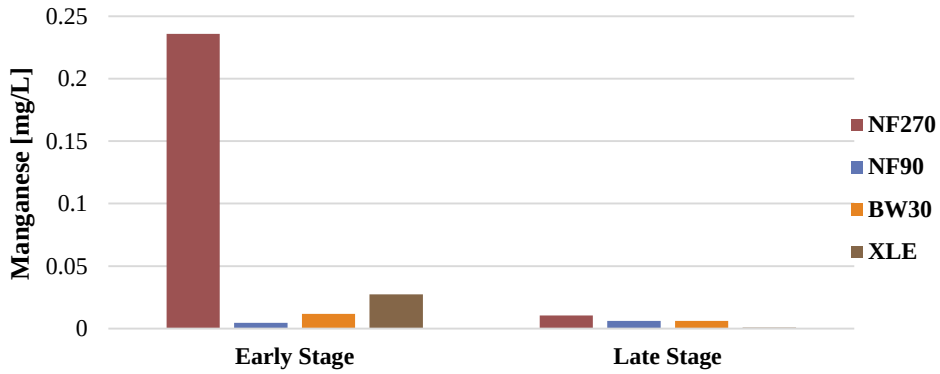


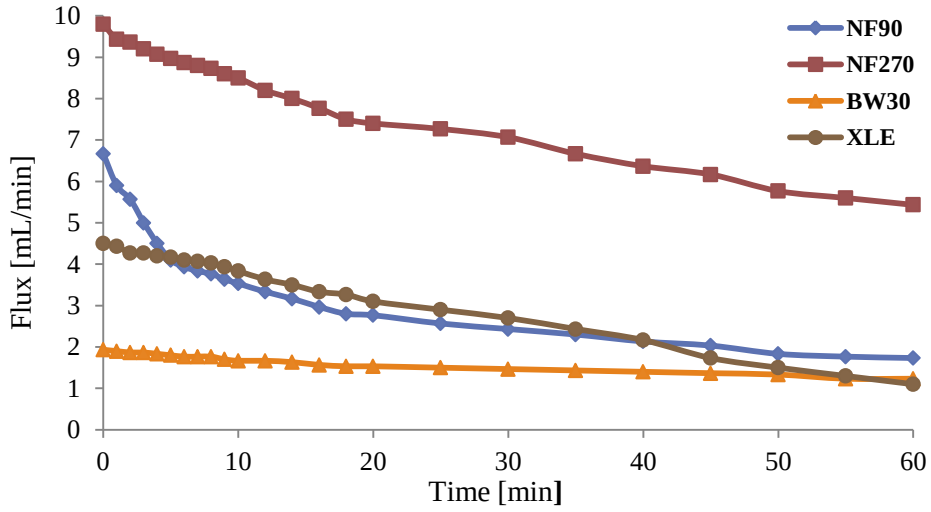
Figure 8: The lab-simulated removal efficiency of manganese at stage 1 and stage 3.



Flux Measurements

A high permeate flux is desirable for Stephenfield to meet the demand of their clients. The high flux of the NF270 makes it a preferable choice while the BW30 had a relatively low flux as observed in Figure 9. However, permeate flux is often inversely proportional to the removal efficiency of soluble material. This idea is supported by Figure 6 through Figure 8 in which the NF270 allowed the significantly larger passage of hardness, alkalinity and DOC than the other three tested membranes. Flux decline due to fouling and/or compaction is another major consideration. The large declines in the NF90 and XLE are explained later.

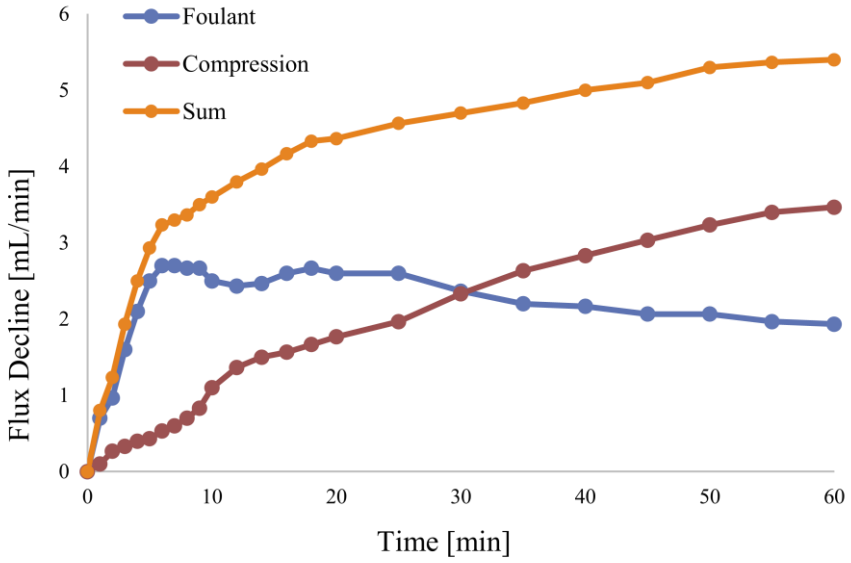
Figure 9: Permeate flux over time.



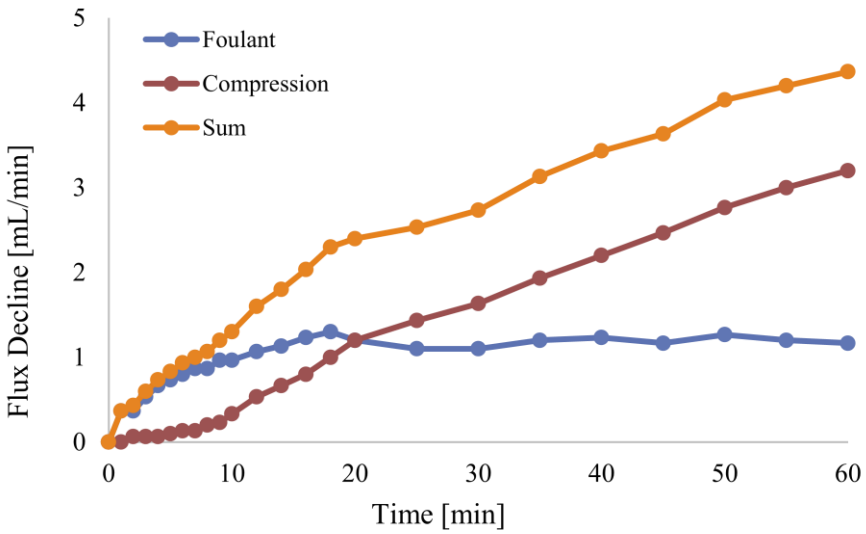
Flux Decline Due to Fouling and Compaction

The effects of membrane compaction were differentiated by subjecting each of the membranes to separate trials containing nanofiltration influent from Stephenfield and deionized water. In all cases, the net effect of flux decline increased over time. A longer test would likely indicate a

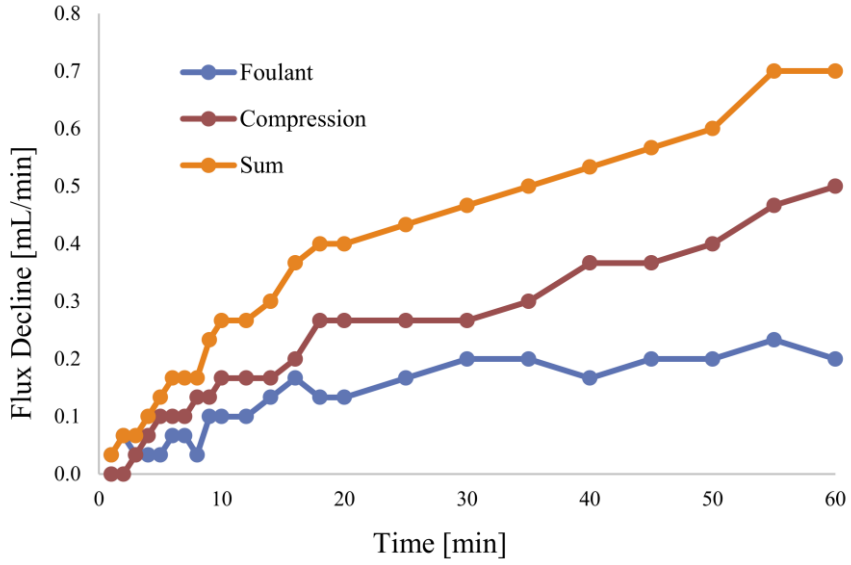
Figure 10: The effects of fouling, membrane compaction and the sum of these two over time for the a) NF90, b) NF270, c) BW30 and d) XLE membranes.



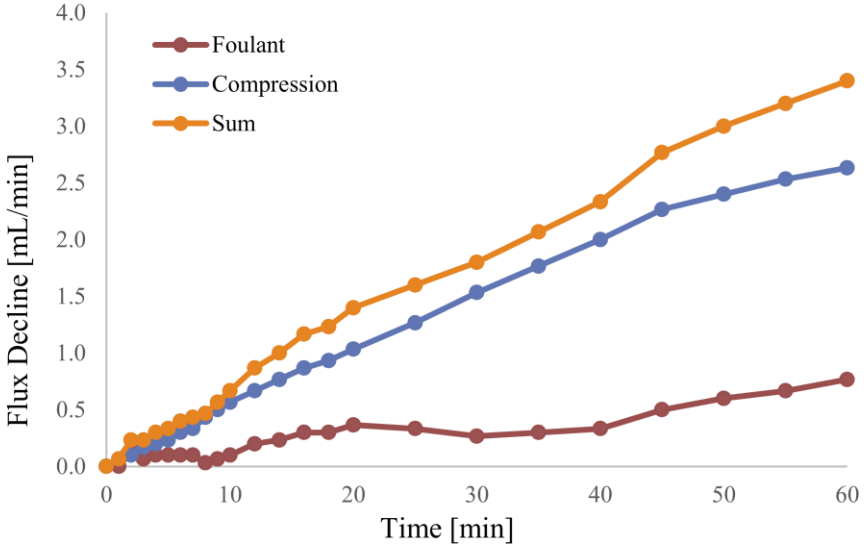
a)



b)



c)



d)

[13]

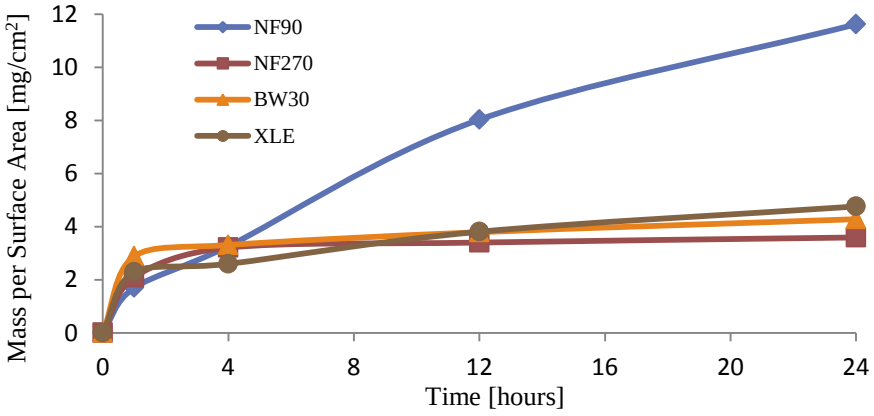
relative maximum. As expected, the effects of fouling were significantly less for the fouling resistant BW30 and XLE membranes; the effects of fouling were approximately three and six times greater for the NF270 and NF90. While the XLE had a relatively high decline in flux, a large part of the decline in flux can be attributed to compaction. This is because the "Xtra Low Energy" membrane is not suitable for high pressures as with the 10bar applied pressure in this experiment.

Unexpectedly, the effects of fouling decreased over time for the NF90 and NF270. This suggests either a change in foulant structure or the physical removal of the attached foulant resulting in the observed flux restoration due to fouling. These results were consistently supported through triplicate trials. A change in foulant structure that would cause the observed flux restoration would be a result of a decrease in foulant density. As the membrane is under a constant applied pressure with overbearing foulant, this relationship is less likely. Focus then shifts to the physical removal of foulant. Scouring is the physical removal of material from a surface due to an applied horizontal shear. The effects of scouring can be observed in the three-dimensional surface scan of the BW30 membrane after 12 hours in Figure 13. The rate of scouring is greater for surfaces with a higher roughness. The proposed relationship between scouring and membrane compaction will be described later.

Retained Mass of Foulant

The NF90 exhibited nearly three times the retained mass of foulant as the other three tested membranes. This is shown graphically in Figure 11. The lack of retained foulant on the BW30 and XLE membranes can be explained by their polyether block amide (commercially sold as PEBAX©) coating. Further investigation regarding the interaction between the polyether block amide and the soluble material in the feed water is necessary. While the NF270 is not coated with the polyether block amide, the lower mass of foulant can be attributed to its relatively smooth surface area which will be discussed in detail in the latter sections of this report.

Figure 11: Retained mass of foulant on the surface of the nanofiltration membrane over the course of 24 hours of operation.



Chemical and Oxidative Testing

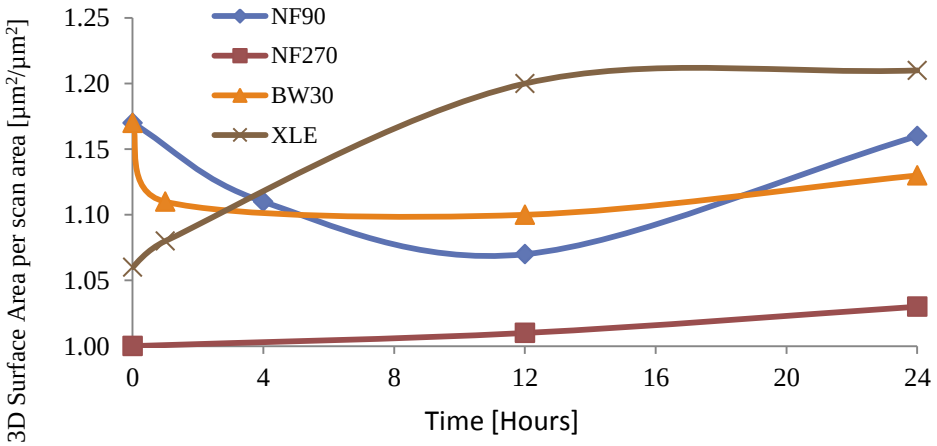
Chemical and oxidative testing was carried out to determine the post-filtration condition of the nanofiltration membranes and to make conclusions about specific foulant characteristics. Three drops of methylene blue dye were placed on each of the four tested membranes at each of the operational times listed in the experimental methods section of this report. As discussed the fouling and compaction section of this report, the XLE membrane is not suitable at the 10bar applied pressure in the experiment which made it the likeliest candidate for post-filtration imperfections. However, in all cases the rinsed dye left no residue on the membrane indicating no visible damage to the active surface of the membranes.

The Fujiwara and acid tests were carried out to determine whether the foulant contained oxidizing halogens and carbonates, respectively. In all cases, these tests failed to show the presence of oxidizing halogens or carbonates.

Surface Complexity

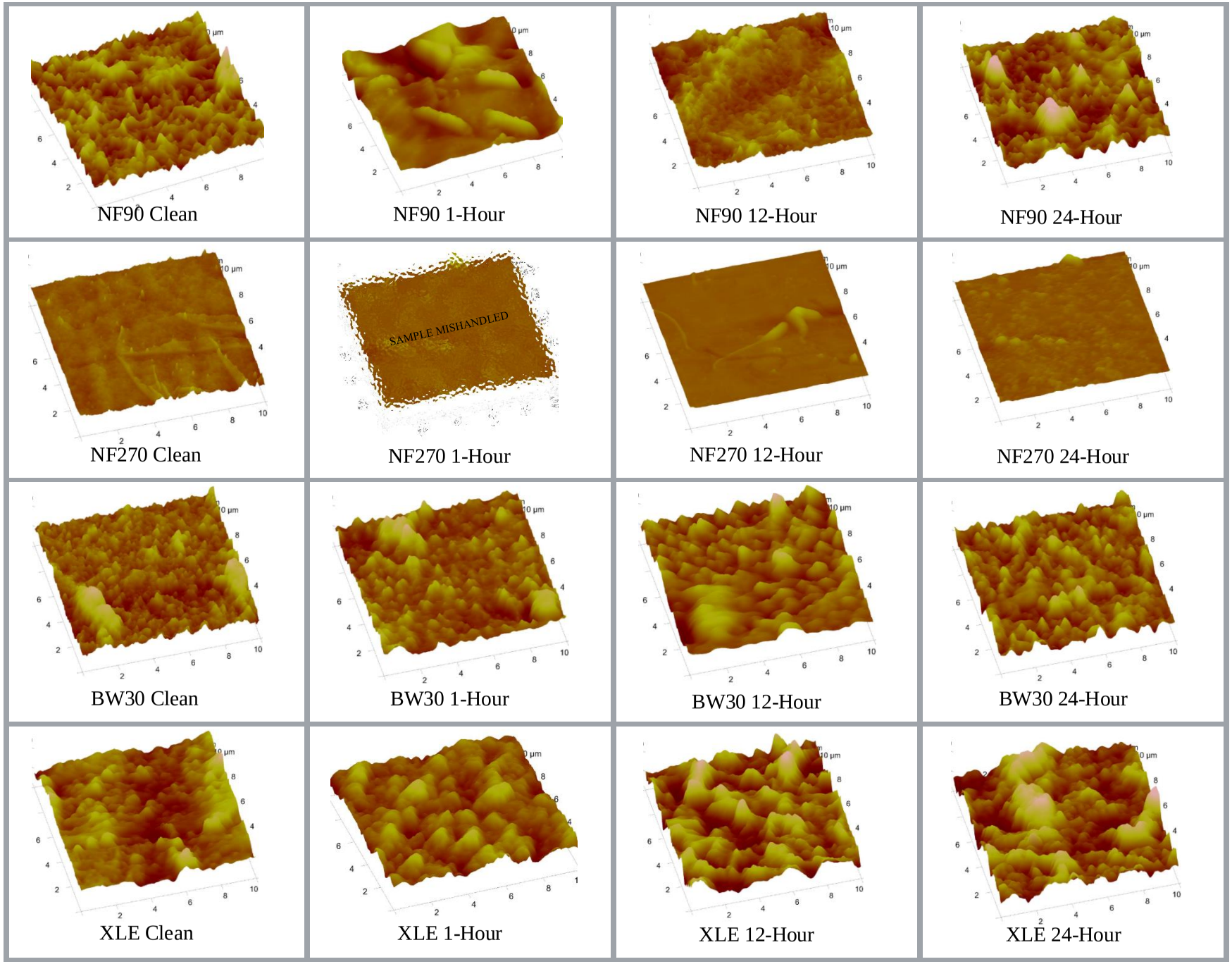
The membrane surface roughness shown in Figure 12 was derived from the three-dimensional surface profiles seen in Figure 13. It is important to note that membrane samples maintained their moisture during scans so as to give the most representative scan of the membrane at the particular operational time.

Figure 12: The change in surface roughness for each of the four tested membranes over time.



Virgin membrane surface roughness appears to be one of the governing factors for the degree of fouling and fouling mechanisms. The initially smooth NF270 and XLE membranes performed as expected: the foulant had accumulated on the surface of the membrane creating steeper peaks and deeper valleys. The initially rough NF90 and BW30 membranes followed the phenomenon labeled “valley clogging” by Vrijenhoek et al. The soluble material in the feed water initially filled in the contours of the membrane which effectively smoothed out the outer surface. It is expected that the rate of membrane fouling is greater during this time period as there is a larger amount of membrane surface area for the foulant to attach and more grab due to the peaks and valleys. This notion of a high rate of fouling is supported by Figure 10 showing the effects of

Figure 13: The Atomic Force Microscopy (AFM) 3-dimensional surface scans for each of the four tested membranes and each of the operational times.



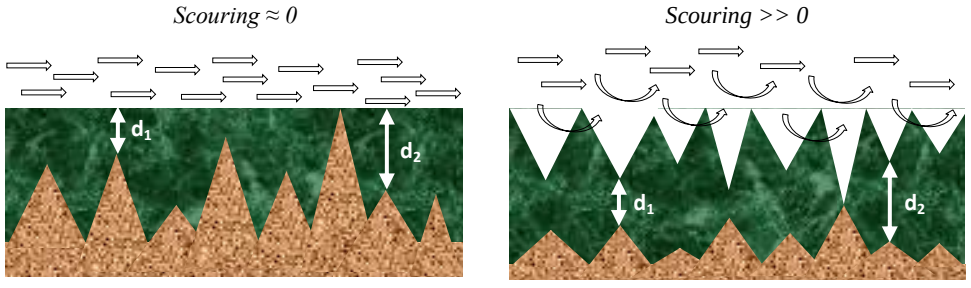
[16]

fouling on the decline in flux. These figures show a greater decrease in flux due to fouling in the early stages of the experiment before showing indications of levelling off after a sufficient period of time. This early decline in flux due to fouling is particularly high for the non-fouling resistant, initially rough NF90 membrane. From this point, the foulant complexity had increased in a similar manner to the NF90 and XLE membranes.

Another crossflow membrane filtration phenomenon, known as scouring, can be observed in the 12-hour AFM scan for the BW30 membrane as seen in Figure 13. Under the crossflow conditions of the experiment, horizontal shear is given by the water under the applied 10bar pressure. The effects of scouring can be used to explain the decrease in the effects of fouling for the NF90 and NF270 in Figure 9a and Figure 9b. As foulant is scraped off the surface, some of the lost flux due to fouling is restored.

Scouring is a potential explanation for the flux restoration due to fouling, but what would occur if the experiment was to continue? Would the effect of fouling on flux for the NF90 and NF270 eventually reach zero? It can be predicted that, in the long run, the addition of foulant by filtration and the removal of foulant by scouring will reach equilibrium. A more important consideration is to when this equilibrium will occur. Given all other variables held constant during the experiment, a possible explanation is a relationship between compaction and fouling. Consider the rough surface of the NF90 covered by a thin layer of foulant making the surface entirely smooth. A schematic of this can be seen in Figure 14a. At a later point in the experiment after membrane compaction has occurred, the foulant complexity has changed. This can be seen in Figure 14b. In both cases, the mass of foulant has been conserved and distance from the surface of the membrane to the surface of the foulant has also been conserved.

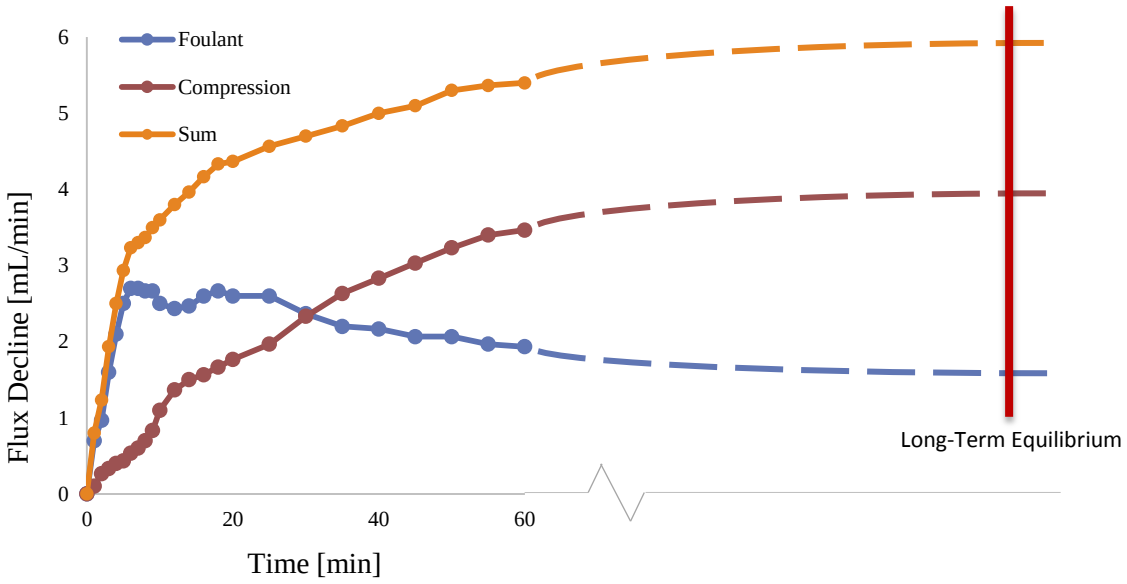
Figure 14: The predicted method for the relationship between flux decline due to fouling and flux decline due to compaction. a) A membrane with a high virgin surface roughness with smooth layer of foulant and b) the same membrane after compaction has occurred.



a) b)

The reduction of peak height of the membrane has effectively pulled in the layer of foulant causing a change in the surface complexity. The resultant surface has a greater roughness to which scouring is more likely to occur. The predicted long-term relationship between the effects of fouling and compaction can be seen in Figure 15. Further investigation regarding this claim will be done at a later date.

Figure 15: The predicted long-term flux decline over time due to fouling and membrane compaction.



Conclusions

Based on the results as a whole, it is clear to see that membrane performance is heavily influenced by the characteristics of the feed water and the properties of the membrane. The NF270 had the lowest removal efficiency of hardness, alkalinity and manganese, but the highest overall flux. The BW30 showed the lowest flux over time and the NF90 experienced the largest degree of flux decline. Three-dimensional surface profiling of the tested membranes over time suggests a unique relationship between initial surface complexity and fouling patterns. The latter parts of this section will provide an explanation for the observed changes in membrane and foulant characteristics over time.

Each membrane was tested for their removal efficiencies of DOC, hardness, alkalinity and manganese. As expected, the membrane with the greatest manufacturer-specified pore size, the NF270, allowed a significantly greater passage of ionic species and manganese. The suffix -270 in the NF270 is a relative indication of pore size. By the same description, the pores of the NF90 and BW30 are three and nine times smaller than the NF270. The removal efficiencies of DOC are roughly the same between all membranes. The passage of potentially large and complex DOC is expected to be lower than the relatively small ionic species. Subsequent testing will be conducted at a later date to determine exact pore size; this will be done by subjecting the membrane to different solutions containing a single, known molecular weight and observing the passage of this carbon (otherwise known as molecular weight cutoff testing). That being said, water treatment plant effluent for general consumer purposes maintains a residual hardness and alkalinity. At roughly 50mg/L $CaCO_3$ for hardness and 100mg/L $CaCO_3$ for alkalinity, the NF270 would not require post-treatment addition of hardness and alkalinity as the other three membranes. However, this comes at the cost of excessive manganese residual in the effluent – an important consideration for membrane selection of the plant operators at Stephenfield due to the relatively high levels of manganese in the surface water.

The observed fouling mechanism for membranes with low virgin membrane surface roughness is very different than the observed fouling mechanism for membranes with high virgin surface roughness. In this experiment, low virgin surface roughness membranes are epitomized by the NF270 and XLE membranes and high virgin surface roughness membranes are epitomized by the NF90 and XLE. Roughness measurements were derived from the AFM scans by taking the ratio of three-dimensional surface area to two-dimensional scan area. In the order of increasing virgin membrane surface roughness: the accumulation of foulant on the NF270 was low due to the nearly-flat surface of the membrane. This smoothness left the foulant with less surface area to attach to or ridges to get caught in. The accumulation of foulant on the XLE membrane followed a similar trend as the NF270 membrane, but increased in surface roughness much faster. This steeper incline in surface roughness can be attributed to the foulant having more surface area to attach to and more valleys to get caught in. The NF90 and BW30 membranes performed very differently. Instead of solely increasing in surface complexity, these membranes began the experiment with high virgin surface roughness, declined in roughness from 0 to 12 hours and experienced an increase in roughness after 12 hours. This is a result of what Vrijenhoek et al. described as valley clogging – the deposition of foulant in the cracks and valleys of the membrane and often leads to a rapid decline in flux. Once the valleys have been sufficiently smoothed out, the surface complexity from further deposition of foulant will increase. Degree of fouling and subsequent flux inhibition can have an important impact on the decline in flux.

The retained mass of foulant appears to be influenced by presence of a fouling-resistant polyether block amide compound. The BW30 and XLE membranes, coated with one of these compounds, exhibited a much lower flux decline due to fouling. The XLE experienced twice as much flux decline due to fouling as the BW30, but roughly one third and one sixth that of the NF270 and NF90, respectively.

Given the information above, as well as other plant operator considerations, the NF270 membrane was selected for pilot-scale testing in September 2015. This membrane was selected for its high permeate flux, low degree of fouling and residual hardness and alkalinity. The performance of the NF270 was monitored for the following two months and failed to meet the effluent goals for manganese content. At the discretion of the plant operators, the stage 2 and stage 3 membranes were swapped out for NF90 membranes to improve the overall removal efficiency of manganese. Pilot-scale performance with the new membrane configuration is under constant monitoring.

Future Projects

Although the experimental results explain some of the key components of nanofiltration membrane fouling, further research is required in order to develop a more complete understanding. One of the tested membranes was a polypiperazine thin-film composite, the NF270, unlike the polyamide thin-film composition of the other three. This membrane featured a smoother surface, higher flux and lower removal efficiency of soluble material. Further research will be conducted to compare the performance of the polyamide and polypiperazine thin-film composites. Further to this membrane property, virgin membrane hydrophobicity and zeta potential will be tested and compared between the membranes with and without the fouling-resistant polyether block amide compound to show any trends between these and fouling patterns. The conducted experiment gave an indication of the short-term effects of both fouling and compaction, but failed to prove the long-term effects. A longer experiment will be conducted

to determine the relative long-term equilibrium point between fouling and compaction and observe any notable relationship between fouling and compaction. Further to this, membrane samples will be subjected to 1, 4, 12 and 24 hours of filtration with DI water and analyzed with atomic force microscopy to show the isolated effects of membrane compaction over time. A more thorough analysis of the foulant will be conducted to identify the composition and further analyze the specific relationship between membrane and foulant. Techniques include, but are not limited to, Fourier transform infrared spectroscopy, fractal analyses, small-angle neutron scattering, cross-section splicing and scanning/transmitting electron microscopy. Plant monitoring and optimization of the developing Stephenfield Regional WTP is expected to continue until project completion.

REFERENCES

Vrijenhoek, Eric M. and Seungkwan Hong and Menachem Elimelech (2001), "Influence of membrane surface properties on initial rate of colloidal fouling of reverse osmosis and nanofiltration membranes", *Journal of Membrane Science Volume 188*, February, pp.115-128.

Jiraratananon, R. and D. Sampranpiboon and R.Y.M. Huang (2002), "Pervaporation separation and mass transport of ethylbutanoate solution by polyether block amide (PEBA) membranes:, *Journal of Membrane Science Volume 210 Issue 2*, pp389-409.

Malvialle, Joël and Peter E. Odendaal and Mark R. Wiesner (1996), "Water Treatment Membrane Processes", American Water Works Association, ed. New York, NY, McGraw-Hill.

Schäfer, A.I, A.G Fane, T.D Waite (2001), "Cost factors and chemical pretreatment effects in the membrane filtration process of waters containing natural organic matter", *Water Research Volume 35 Issue 6*, pp.1509-1517.

Katsuki, Kimura et al. (2004), "Irreversible membrane fouling during ultrafiltration of surface water", *Water Research Volume 38 Issure 14-15*, pp.3431-3441.

Persson, Kenneth M. and Vassilis Gekas and Gun Trägårdh (1995), "Study of membrane compaction and its influence on ultrafiltration water permeability", *Journal of Membrane Science Volume 100 Issue 2*, pp.155-162.

Louis, Jennifer S. et al. (2006), "Effects of polyether-polyamide block copolymer coating on performance and fouling of reverse osmosis membranes", *Journal of Membrane Science Volume 280 Issue 1-2*, pp.762-770.